Translational Oncology
www.transonc.com

Volume 12 Number 10 October 2019 pp. 1314–1322 **1314**

Orally bioavailable glutamine antagonist prodrug JHU-083 penetrates mouse brain and suppresses the growth of MYC-driven medulloblastoma[1,2]

Allison R. Hanaford[*], Jesse Alt[†], Rana Rais[†,‡], Sabrina Z. Wang[*], Harpreet Kaur[*], Daniel L.J. Thorek[§,¶], Charles G. Eberhart[#,], Barbara S. Slusher[†,‡], Allison M. Martin[*,**] and Eric H. Raabe[*,#,**]**

[*]Division of Pediatric Oncology, Johns Hopkins University School of Medicine, Baltimore, MD; [†]Johns Hopkins Drug Discovery, Johns Hopkins University School of Medicine; [‡]Department of Neurology, Johns Hopkins University School of Medicine; [§]Mallinckrodt Institute of Radiology, Washington University School of Medicine, St. Louis, MO; [¶]Department of Biomedical Engineering, Washington University, St. Louis, MO; [#]Department of Pathology, Johns Hopkins University, School of Medicine, Baltimore, MD 21287; [**]Sidney Kimmel Comprehensive Cancer Center, Johns Hopkins University, School of Medicine, Baltimore, MD 21287

Abstract

A subset of poor-prognosis medulloblastoma has genomic amplification of *MYC*. MYC regulates glutamine metabolism in multiple cellular contexts. We modified the glutamine analog 6-diazo-5-oxo-l-norleucine (DON) to mask its carboxylate and amine functionalities, creating a prodrug termed JHU-083 with increased oral bioavailability. We hypothesized that this prodrug would kill MYC-expressing medulloblastoma. JHU-083 treatment caused decreased growth and increased apoptosis in human MYC-expressing medulloblastoma cell lines. We generated a mouse MYC-driven medulloblastoma model by transforming C57BL/6 mouse cerebellar stem and progenitor cells. When implanted into the brains of C57BL/6 mice, these cells formed large cell/anaplastic tumors that resembled aggressive medulloblastoma. A cell line derived from this model was sensitive to JHU-083 *in vitro*. Oral administration of JHU-038 led to the accumulation of micromolar concentrations of DON in the mouse brain. JHU-083 treatment significantly increased the survival of immune-competent animals bearing orthotopic tumors formed by the mouse cerebellar stem cell model as well as immune-deficient animals bearing orthotopic tumors formed by a human MYC-amplified medulloblastoma cell line. These data provide pre-clinical justification for the ongoing development and testing of orally bioavailable DON prodrugs for use in medulloblastoma patients.

Translational Oncology (2019) 12, 1314–1322

Address all correspondence to: Eric H. Raabe, MD, PhD, Bloomberg Children's Center Rm 11379, Johns Hopkins Hospital, 1800 Orleans Street, Baltimore, MD 21287. E-mail: eraabe2@jhmi.edu
Address all correspondence to: Allison M. Martin, MD, Pediatric Hematology/Oncology, Albert Einstein College of Medicine, 1300 Morris Park Avenue, Van Etten 6A04B, Bronx, NY, 10461 E-mail: allison.martin@einstein.yu.edu
[1] Funding support: NINDS 1R01NS103927 (BSS and EHR); NCI R01 R01CA229451 (BSS), Alex's Lemonade Stand Foundation and the Swifty Foundation (EHR and BSS); Children's Cancer Foundation (EHR and BSS); The Spencer Grace Foundation (EHR), The Ace for a Cure Foundation (EHR); Beez Foundation (AMM); Giant Food Pediatric Cancer Research Fund; National Cancer Institute Core Grant to the Johns Hopkins Sidney Kimmel Comprehensive Cancer Center (P30CA006973).

Introduction

Medulloblastoma is the most common malignant brain tumor of childhood. Though 60% of medulloblastoma patients survive for at least 10 years, survival varies widely depending on the molecular genetics of the patient's tumor [43]. RNA expression profiling and DNA methylation studies have subdivided medulloblastoma into at least four molecular subgroups: WNT, SHH, Group 3, and Group 4 [25,33]. The standard treatment for medulloblastoma is surgical resection of the tumor, radiation and chemotherapy. This therapy is associated with high morbidity; medulloblastoma patients often experience cognitive delays, learning disabilities, hearing loss, increased risk for future malignancies and stroke, endocrine dysfunction, and cerebellar mutism syndrome [5,15,16,24,39,44]. A subset of patients within Group 3 have amplification or over-expression of the *MYC proto*-oncogene. These patients have among the worst clinical outcomes of all medulloblastoma patients [2,7]. The relatively poor prognosis for many medulloblastoma patients and the severe complications faced by survivors indicate an urgent need for more effective and less toxic therapies.

MYC regulates a variety of cellular processes, including metabolism of both glucose and the amino acid glutamine [9]. Glutamine is the primary nitrogen source for synthesis of nucleic acids, other amino acids, and hexosamines. Glutamine can also be used as a carbon source to replenish TCA cycle intermediates, in a process called glutaminolysis [27,31]. Many types of MYC-driven cancers uptake large quantities of glutamine, some to the point of becoming "addicted" and being unable to survive without glutamine [10,12,26,47]. MYC regulates the utilization of glutamine by upregulating genes involved in glutamine uptake and metabolism, ASCT2, LAT-1 and glutaminase (GLS) [4,18].

The role of glutamine metabolism in MYC-driven medulloblastoma is underexplored, but a study by Wilson *et al* [46] supports the hypothesis that a subset of medulloblastoma tumors have elevated glutamine metabolism. Wilson *et al* non-invasively measured glutamate levels in the tumors of medulloblastoma patients using magnetic resonance spectroscopy (MRS). They found that patients with high-levels of glutamate in their tumors had much poorer survival than patients with low glutamate levels. The initial step in glutamine metabolism is the conversion of glutamine to glutamate by GLS. High levels of glutamate indicate that glutamine is being metabolized at a high level. Thus, increased glutamine metabolism is associated with poor-prognosis medulloblastoma. Because glutamine metabolism is a potential therapeutic target in other MYC-driven cancers [11,48], we hypothesized that targeting glutamine metabolism in MYC-driven medulloblastoma could be a potentially useful strategy in this devastating tumor type.

Methods

2.1 JHU-083

The synthesis of JHU-083 (Ethyl 2-(2-Amino-4-methylpentanamido)-DON) was conducted as detailed by our group previously [37]. For *in vitro* testing, JHU083 was dissolved in sterile water; for *in vivo* studies it was dissolved in sterile PBS buffer. JHU-083 doses in this paper are given as the DON-equivalent dose. Due to the presence of the promoities, 1.83 mg of JHU-083 equals 1.0 mg of unmodified DON.

2.2 Cell Culture

The patient-derived medulloblastoma cell line D425MED was established at Duke University [21]. It is grown in MEM media supplemented with 10% FBS. We generated human neural stem cell models of MYC-driven medulloblastoma or SV40 immortalized control cells as described [20]. Our MYC-expressing models recapitulate Group 3, MYC amplified medulloblastoma by expression profiling and phenotype [20]. These human neural stem cell lines grow as neurospheres in "EF" media composed of 30% Ham's F12, 70% DMEM, 1% antibiotic antimycotic, 2% B27 supplement, 5ug/mL heparin, 20 ng/mL EGF, and 20 ng/mL FGF2 [20]. Those harboring AKT are grown under puromycin selection. The MED211 patient derived xenograft was obtained from the Brain Tumor Resource Lab and is described in [6]. A cell line was derived from this PDX model by removing tumor tissue from tumor-bearing mice at the time of sacrifice and passing tumor through a P1000 pipette. Cells were grown in EF media. All cells were verified to be mycoplasma free by PCR testing. Cell line identity testing was performed by the Johns Hopkins Genetic Resources Core Facility and is included in Supplemental Figure 1.

2.3 Mouse Medulloblastoma Model

Creation of this model is described in detail in the main body of the manuscript. The cells are grown in EGF/FGF media made with a 50:50 mixture of F12:DMEM, but is otherwise identical to that described above. The R248W-TP53 plasmid (Addgene plasmid 16437) and MYC plasmid (Addgene plasmid 17758) were subcloned into pWPI (Addgene 12254) [29]. Lentivirus was produced by transfecting 293T cells with VSV-G envelope plasmid, Δ8.9 gag/pol plasmid and the plasmid containing the gene of interest as described in [36] using Fugene (Roche) per manufacturer's instruction. The supernatant was collected at 48 and 72 h. The collected supernatant was filtered with a 0.45 micron filter and concentrated overnight at 4'C using 5% PEG 8000 and 150 mM NaCl then centrifuged for 30 minutes at 2000xg. Concentrated virus was stored at -80C in serum free DMEM until use. Visualization of the distribution of this model *in situ* was provided by fluorescence imaging macroscopy using a dual camera setup for GFP and white light (anatomical) imaging. The excised brain was illuminated by a SpectraX LED light source (Lumencor) with emission light captured by an F1.2 80 mm lens (Nikon), and filtered by a dichroic and low pass filter in an OptosplitII (Cairn) tube to dual Pixelfly CCDs (PCO). Data was acquired in Metamorph NX.

2.4 Cell growth Assay

Experiments were performed in 96 well plates. Equal numbers of cells were plated in triplicate for each treatment. 20uL of CellTitre 96 Aqueous One Solution (Promega) was added to each well for every 100uL of media and incubated at 37C for 1 hour. Absorbance was read at 490 nM on a plate reader. Growth between vehicle and drug treated cells was statistically analyzed using Student's *t*-test.

2.5 Western blots

Protein was extracted from cell pellets using RIPA buffer and quantified using a Bradford Assay. Antibody against cleaved-PARP is from Cell Signaling technologies (#9541). Antibodies against ACTIN (sc-47778) and MYC (sc-40) are from Santa Cruz Biotechnologies. The following dilutions were used cleaved-PARP (1:800), ACTIN (1:1000), and MYC (1:1000). Peroxidase labeled secondary antibodies are from

Cell Signaling Technologies and used at a 1:3500 dilution. Bands were quantified using ImageJ.

2.6 Cleaved Caspase-3 immunofluorescence

Following 72 h drug treatment, cells were fixed in cytospin fluid and spun onto glass slides using a cytocentrifuge. Cells were permeabilized in 0.1% TritonX, blocked in 5% normal goat serum, and incubated with anti-cleaved caspase-3 antibody diluted 1:400 (Cell Signaling Technology®, clone 5A1E), followed by a secondary antibody conjugated to Cy3 diluted 1:500 (Jackson ImmunoResearch). DAPI was used as a counterstain. Three DAPI and the corresponding Cy3 images were taken for each slide. The number of DAPI and Cy3 positive cells were counted using Adobe® Photoshop®. For each pair of images, the percent of Cy3 positive cells was calculated. The average Cy3 positivity was determined by calculating the average of at least three pairs of images for each treatment. Images were blinded before counting. Vehicle and drug treated cells were compared by Student's t-test.

2.7 Histology

Brains were fixed in 10% buffered formalin for a minimum of 24 h. The Johns Hopkins Pathology Reference Lab processed tissue for paraffin embedding and sectioning.

2.8 Immunohistochemistry

All IHC staining was performed by the Johns Hopkins Oncology Tissue services.

2.9 Animal Studies

Xenografting was conducted in female mice of a minimum of 6 weeks old. D425MED cells were injected into nude (Nu/Nu) mice. mNSC DNp53 MYC cells were injected into C57BL/6J mice. Prior to implantation of cells, animals were anesthetized using a mixture of 10% ketamine and 5% xyaline. A burr hole was made in the skull 1 mm to the right and 2 mm posterior of the lambdoid suture with an 18 gauge needle. The needle of a Hamilton syringe was inserted 2.5 mm into the brain using a needle guard and 100,000 D425MED cells or 50,000 mCB DNp53 MYC in 3uL of media were injected into the cerebellum. JHU-083 was prepared in sterile PBS and administered by oral gavage in a 100uL bolus twice weekly on Tuesdays and Fridays. Animals were monitored daily. Individuals showing signs of neurologic impairment or increased intracranial pressure were euthanized, brains removed and fixed in formalin. Survival curves were analyzed using a Log-rank test. For the JHU-083 brain penetration pharmacokinetic study, five athymic nude mice without brain tumors were given a single DON-equivalent dose of 20 mg/kg JHU-083 dissolved in PBS by oral gavage. Exactly 1 h post dose, mice were euthanized and the brain regions manually dissected and flash frozen. Dosing of the animals was staggered to ensure each animal was only exposed to the drug for 1 h. Extraction and quantification of DON was performed as described in [49].

2.10. Study Approval

For animal care and anesthesia, "Principles of laboratory animal care" (NIH publication No. 8623, revised 1985) was followed, using a protocol approved by the Johns Hopkins Animal Care and Use Committee, in compliance with the United States Animal Welfare Act regulations and Public Health Service Policy.

Results

3.1 JHU-083

To investigate the utility of glutamine metabolism as a therapeutic target in MYC-driven medulloblastoma, we utilized JHU-083 (Ethyl 2-(2-Amino-4-methylpentanamido)-DON), a dual promoeity prodrug of the glutamine analog 6-diazo-5-oxo-l-norleucine (DON). JHU-083 is orally bioavailable and converts to DON after administration (Figure 1) [37] [49].

3.2 A cell-based mouse model of MYC-driven medulloblastoma

In addition to utilizing existing patient-derived medulloblastoma cell lines, we created a novel mouse model using mouse cerebellar stem and progenitor cells to facilitate *in vivo* studies in the context of an intact immune system (Figure 2A). The developing cerebellum was dissected out of E15 C57BL/6J fetuses, the tissue manually dissociated and placed in EGF/FGF containing, serum-free cell culture media. These cells grow as neurospheres. The isolated stem and progenitor cells were infected with lentivirus bearing human dominant-negative TP53 (DNp53) and human MYC, both of which are associated with aggressive, poor-prognosis medulloblastoma [7,33]. To generate subclones, individual neurospheres were manually selected with aid of a dissecting microscope and expanded before the expression of MYC and P53 was verified by western blot. A representative sub-clone (Figure 2B) shows robust expression of both MYC and TP53. Sub-clones positive for both oncogenes were injected into the cerebella of 4–6 week old adult female C57BL/6J mice. If a subclone formed a tumor, the tumor was implanted into additional mice. This *in vivo* passaging was repeated five times. A cell line was generated from the fifth passage. The tumors formed from mCB DNp53 MYC cells resemble human anaplastic medulloblastoma, with leptomingeal dissemination (Figure 2C, D) as well as a large cell/anaplastic phenotype Figure 2E, F) [14]. These tumors also showed very robust expression of MYC (Figure 2G) and TP53 (2H) by IHC, similar to group 3 MYC-driven medulloblastoma [20].

3.3 JHU-083 reduces growth of MYC-expressing medulloblastoma cell lines

Treatment with 10uM of JHU-083 significantly reduced the growth of MYC-expressing medulloblastoma models as measured by MTS assay (Figure 3). All the cell models tested, except for human neural stem cells immortalized with SV40, express robust amounts of MYC (Figure 3A).

In the patient derived, MYC-amplified cell line D425MED, 10uM JHU-083 treatment decreased growth by 80% at day 5 of treatment

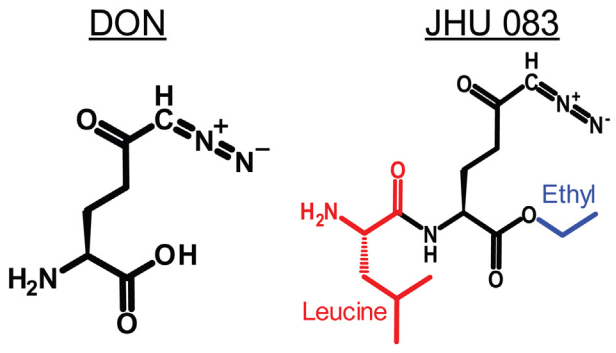

Figure 1. Chemical structure of 6-diazo-5-oxo-l-norleucine (DON) and the prodrug JHU-083 (Ethyl 2-(2-Amino-4-methylpentanamido)-DON).

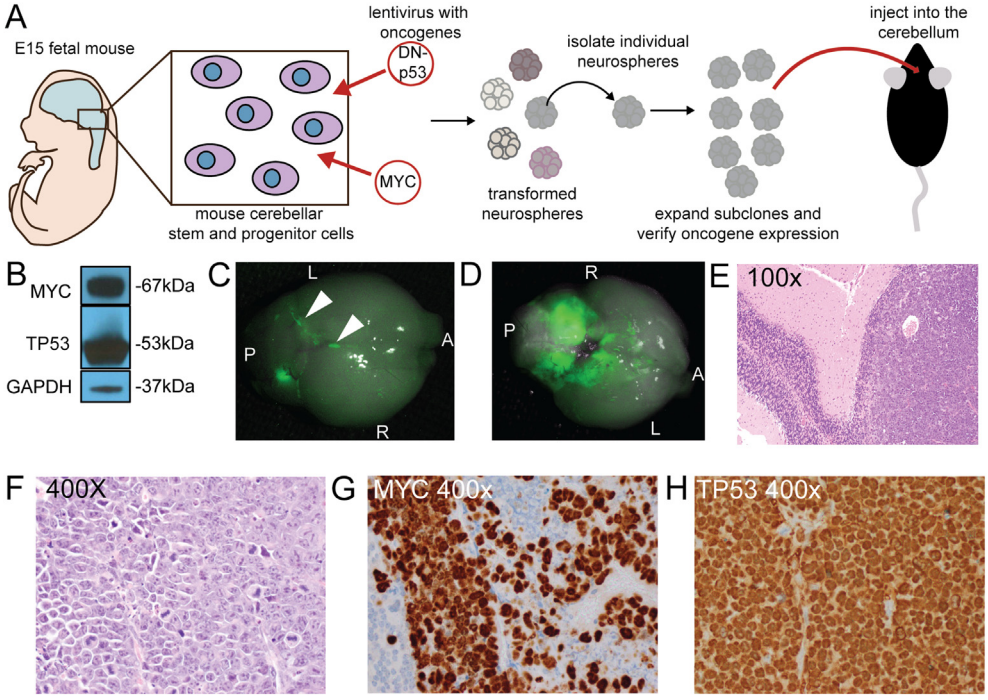

Figure 2. Development and characterization of a mouse model of MYC-expressing medulloblastoma. A. Diagram showing the steps in model development. Mouse stem and progenitor cells were isolated from the developing mouse cerebellum and dissociated and expanded in culture. They were then transduced with lentiviruses containing c-MYC and R248WTP53 (DNp53). GFP + clones were selected and expanded for further characterization. B. Western blot showing the expression of the introduced oncogenes in the subclone used in this paper. C. Whole mount fluorescence microscopy showing the dorsal view of tumor formed by GFP-positive mCB DNp53 MYC cells, with arrowheads highlighting leptomeningeal spread of GFP + cells. A = anterior P = posterior R = right L = left D. Ventral view of the same brain, showing extensive involvement of the cerebellum with spread to the adjacent brain. E. Hematoxylin and eosin (H and E) staining at low power showing the tumor formed by mCB DNp53 MYC cells (right) adjacent to normal cerebellum (left). F. High-power H and E showing characteristics of MYC-driven medulloblastoma including abundant mitoses and apoptotic bodies, as well as large cell/anaplastic phenotype as demonstrated by prominent nucleoli and nuclear wrapping. G. IHC for MYC, showing robust expression (brown stain). Tumor cells are positive and surrounding normal cells serve as an internal negative control. H. IHC for TP53, showing robust expression (brown stain). Blood vessel at center left of panel serves as an internal negative control.

(P = 0.00016) (Figure 3B). In human cerebellar neural stem and progenitor cells transformed by MYC alone, 10uM JHU-083 treatment caused a 98% decrease in growth at day 7 of treatment ($P = 5.2x10^{-6}$). Human neural stem and progenitor cells transformed with dominant negative TP53, human telomerase (hTERT), AKT and MYC form tumors that phenocopy large cell/anaplastic human medulloblastoma when injected into the cerebella of nude mice. This model also mimics the expression profile of the C1 subgroup of medulloblastoma, the subgroup with the poorest prognosis that consists of MYC-expressing tumors [20]. In two subclones created by the addition of dominant-negative TP53, hTERT, constitutively-active AKT, and MYC to human cerebellar stem and progenitor cells, 10uM JHU-083 reduced growth at day 7 by 55% in #2 ($P = 3.5x10^{-5}$, Figure 3D) and by 50% in #5 (P = 0.03, Figure 3E). JHU-083 treatment significantly decreased the growth of mouse cerebellar stem and progenitor cells transformed with MYC and dominant-negative TP53 (Figure 3F). 72 h treatment with 10uM JHU083 lead to an 86% reduction in growth by day 4 of treatment ($P = 7.23x10^{-6}$).

3.4 JHU-083 treatment increases apoptosis in MYC-expressing medulloblastoma cell lines

Treatment with 10uM JHU-083 for 24 h caused an average 3.5-fold increase in the expression of cleaved-PARP as measured by Western blot in five MYC-expressing medulloblastoma cell lines (Figure 4A), indicating that JHU-083 treatment induces apoptotic cell death. Treatment with 10uM or 20uM of JHU-083 for 72 hours similarly caused a significant increase in the percentage of cleaved caspase-3 positive cells as measured by immunofluorescent staining (Figure 4B). In the patient-derived cell line D425MED, 10uM and 20uM of JHU-083 increased the percentage of cleaved caspase-3 positive cells from 3% to 14% ($P = 1.99x10^{-}6$) and 29% ($P = 1.9x10^{-}7$) respectively.

We generated the MED211 cell line from a medulloblastoma patient-derived xenograft (PDX) tumor. Genetic analysis indicates that this PDX has *MYC* amplification and belongs to the G3 medulloblastoma subgroup [6]. In MED211 cells, treatment with 10uM or 20uM JHU-083 increased the percentage of cleaved caspase-3 positive cells from a baseline level of 22% to 64% (P = 6.2x10–10) and 75% (P = 2.4x10–11). In human cerebellar neural stem cells transformed with MYC alone, 10uM and 20uM of JHU-083 increased cleaved caspase-3 levels from 22% to 32% (P = 0.03) and then to 47% ($P = 1.^{5}x10^{-}5$). In CB DNp53 hTERT AKT MYC #2, 10uM JHU-083 and 20uM JHU-083 increased cleaved caspase-3 levels from 8% to 22% ($P = 8.2x10^{-8}$) and 41% ($9.7x10^{-9}$). In CB p53 hTERT AKT MYC #5, 10uM JHU-083 and 20uM JHU-083 increased cleaved caspase-3 levels from 12% to 30% (P = 0. 0002) and 47% ($P = 2.9x10^{-5}$). In the mouse medulloblastoma cell line mCB TP53 MYC, 10uM JHU-083 and 20uM JHU-083 increase cleaved caspase-3

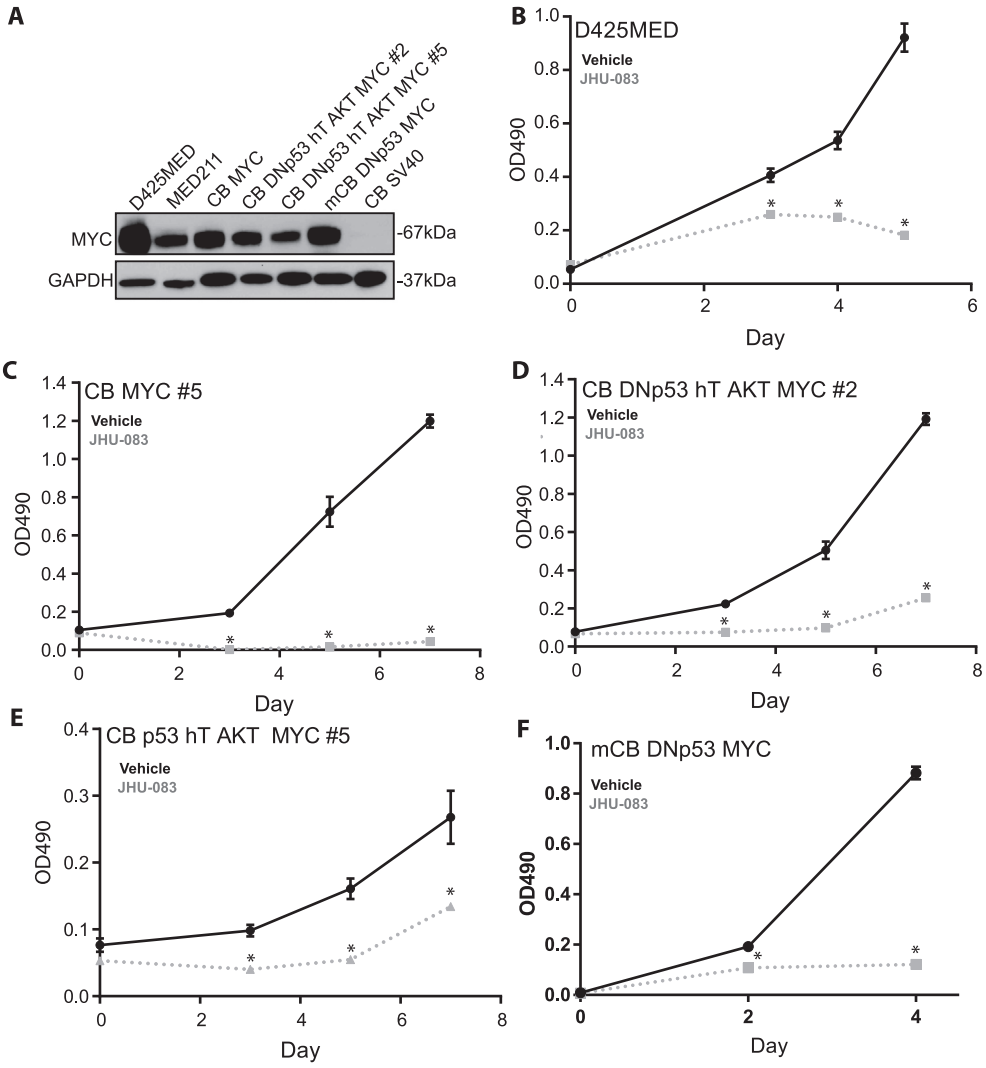

Figure 3. JHU-083 decreases growth of MYC-expressing medulloblastoma cell lines. A. Western blot showing robust MYC expression of the cell lines used in this manuscript. Human cerebellar stem cells immortalized with SV40 are negative. B-F. MTS growth assays showing decreased growth of multiple cell lines expressing MYC. Asterisks indicate P<0.05 by Student"s t-test compared to similar day control. Representative graphs shown. Each experiment was repeated a minimum of 3 times with similar results.

levels from 34% to 50% (P = 2.4x10^{-6}) and 59% (P = 1.5x10^{-7}). Non-MYC expressing human neural stem cells immortalized with SV40 were not sensitive to treatment with JHU-083 at 10uM or 20uM (P >0 .82). These results indicate that JHU-083 induces apoptosis in MYC-expressing medulloblastoma cell lines and has little effect on non-MYC expressing cells. To further address the mechanism of high-MYC cells being sensitive to JHU-083, we determined the expression of glutaminase (GLS) in our neural stem cell models by western blot. GLS is regulated by MYC and is a key enzyme governing the conversion of glutamine to glutamate [8]. We find that cells transduced with SV40 do not express detectable MYC and do not express GLS, while cells transduced with MYC alone or additional oncogenic drivers such as R248WTP53 and activated AKT express robust levels of GLS (Supplemental Figure 2).

3.5 JHU-083 administration achieves micromolar concentrations of DON in the brain

To determine if DON delivered by JHU-083 is capable of crossing the blood–brain barrier, nude mice were administered JHU-083 by oral gavage (20 mg/kg). After 1 hour, the animals were euthanized and the brains removed. The cortex, cerebellum and brain stem were manually separated and flash frozen in liquid nitrogen. DON levels in the brain were subsequently quantified *via* LC–MS/MS as our laboratory has previously described [49]. There was no significant difference in the concentration of DON in the three regions of the brain analyzed (P = 0.42, one-way ANOVA, n = 5) (Figure 5A). The cerebellum had an average concentration of 11.3 μM of DON. Because 10uM JHU-083 successfully reduces growth of MYC-expressing medulloblastoma cell lines (Figure 3) and induces apoptosis (Figure 4), we hypothesized that a 20 mg/kg dose of JHU-083 would significantly extend the survival of animals bearing MYC-expressing medulloblastoma tumors.

3.6 JHU-083 extends the survival of animals with MYC-driven medulloblastoma orthotopic xenografts

Treatment with JHU-083 (20 mg/kg twice weekly) extended the survival of athymic nude mice bearing D425MED orthotopic xenografts from 21 to 28 days, an increase of 29 percent (P = 0.006 by Log-rank

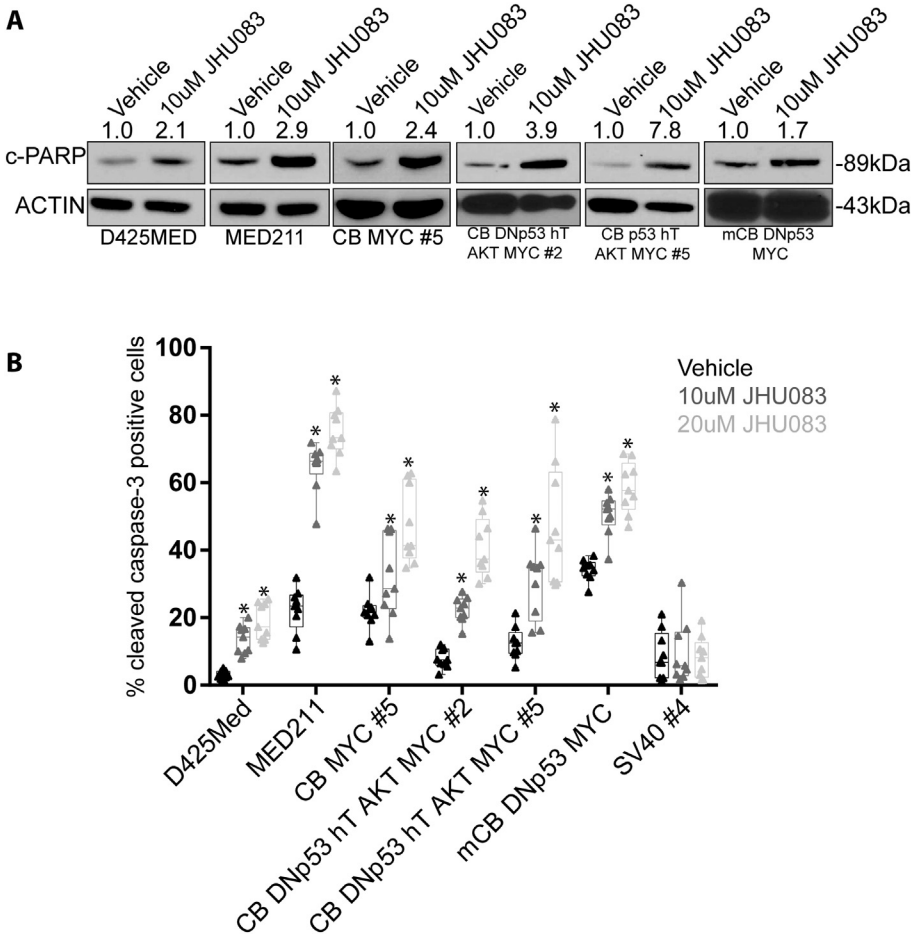

Figure 4. JHU-083 treatment induces cell death by apoptosis. A. 24 h treatment with 10uM JHU-083 causes increased expression of cleaved-PARP as identified by western blot. Numbers above the blot indicate fold-increase of cleaved-PARP expression compared to vehicle control. Cleaved-PARP expression was normalized to ACTIN. B. Graph showing that 72 h treatment with 10uM or 20 uM JHU-083 causes a significant increase in cleaved caspase-3 positive cells as determined by immunofluorescence. Asterisk indicates $P < 0.05$ by Student's *t*-test compared to vehicle control. N = 3 biological replicates. Bars represent min. to max with each replicate result represented by a solid dot.

test) (Figure 5B). Figure 5C shows D425MED tumor adjacent to normal cerebellum.

JHU-083 treatment also successfully extended the survival of C57BL/6 mice with mCB DNp53 MYC orthotopic xenografts (Figure 5D). The twice weekly treatment with 20 mg/kg of JHU-083 extended median survival from 16 days to 25 days, an increase of 43 percent ($P < 0.0001$ by Log-rank test). Figure 5E shows mCB DNp53 MYC tumor adjacent to normal cerebellum.

Discussion

Patients with MYC-expressing medulloblastoma face a grim prognosis. There are currently no biologically informed therapies available for these patients. The experiments presented here show the potential for a metabolic approach to treating this tumor type. The majority of MYC-positive medulloblastoma tumors fall into the G3/C1 subgroup. Other studies have shown that many relapsed medulloblastoma tumors are positive for MYC expression upon relapse, regardless of subgroup [22], suggesting that targeting MYC-regulated metabolism could have utility in recurrent medulloblastoma of other subtypes as well as G3/C1 patients.

A critical aspect of this study is that it compares efficacy of a novel glutamine antagonist against MYC-driven medulloblastoma models of both human and mouse origin and demonstrates a therapeutic response in both immune deficient and immune competent CNS microenvironments. Our mCB DNp53 MYC cells are derived from C57BL/6J mice and are rapidly tumorigenic in immune intact animals. *TP53* mutations and *MYC* amplification are not only associated with poor outcomes in medulloblastoma at diagnosis, they are also the most frequently gained mutations in relapsed medulloblastoma and both are associated with aggressive disease phenotypes [22]. Since novel therapeutics will initially be tested in human patients with relapsed disease and intact immune systems, the mCB DNp53 MYC cells present an ideal system for modeling treatment effects in relapsed medulloblastoma. This model differs from other similar models [35] in that it was established in an immune intact mouse, utilizes human oncogenes to mimic human tumor biology in a mouse cell of origin and in that lentiviral vectors were used to deliver these oncogenes. Since medulloblastoma is an immunologically "cold" tumor [30], lentivirus was used to decrease the risk of potentially immunogenic insertional mutagenesis that can occur with retroviral models [23]. Careful clone selection after *in vivo* adaptation has led to the generation of a stable cell line model of medulloblastoma available for orthotopic use in any transgenic mouse strain developed on the C57BL/6J background, one of the oldest and most widely used mouse strains in biomedical science.

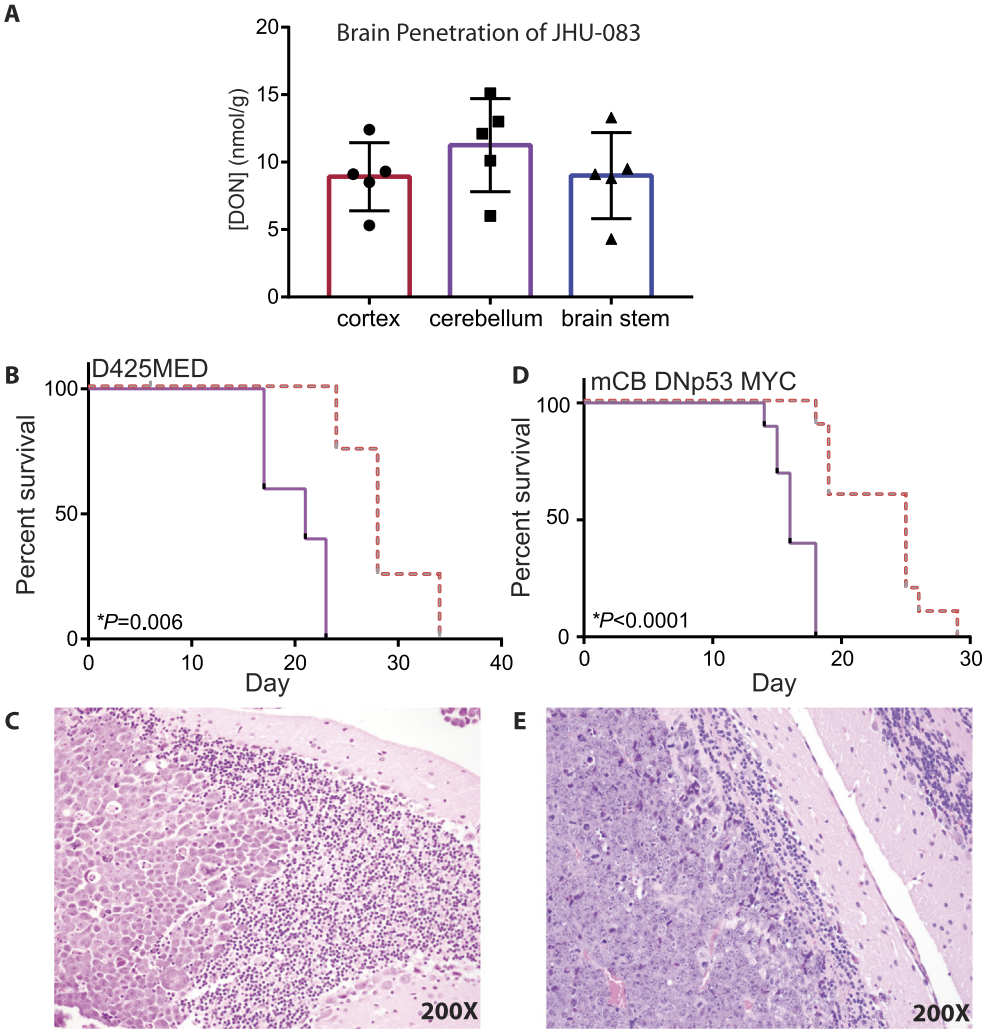

Figure 5. JHU-083 improves survival of mice with medulloblastoma tumors. A. 1 hour after a single dose of 20 mg/kg JHU-083, DON levels are detectable in mouse brain at a range from 8–12 nmol/g. There was no difference in DON levels in the different brain regions. $P = 0.42$ by one-way ANOVA, n = 5 brains. Error bars indicate standard deviation. B. Twice weekly 20 mg/kg dosing of JHU-083 significantly extended the survival of athymic nude mice with D425MED tumors. Dashed red line = JHU-083 Solid purple line = vehicle. $P = 0.006$ comparing treated *vs* vehicle control as determined by Log-rank test. N = 5 animals per group. C. H and E image (200X) of D425MED tumor (left) adjacent to normal cerebellum (right), showing large cell histology associated with group 3 medulloblastoma. D. Twice weekly 20 mg/kg JHU-083 treatment significantly extend the survival of C57BL/6J mice with mCB DNp53 MYC tumors. Dashed red line = JHU-083. Solid purple line = vehicle. $P = 0.0001$ comparing treated *vs* vehicle control as determined by Log-rank test. N = 10 animals per group. E) H and E image (200X) of mCB DNp53 MYC tumor (left) adjacent to normal cerebellum (right).

We observe a similar survival effect of JHU-083 in our immundeficient and immune-intact medulloblastoma models. Although dissecting the effects of DON and DON prodrugs on the adaptive immune system is beyond the scope of this study, we include an immune-competent MYC-driven medulloblastoma model to demonstrate that a therapeutic benefit is preserved in this setting. The dependence of activated lymphocytes on glutamine is well described and reviewed recently by Bettencourt and Powell [3]. DON and JHU-083 have a marked immunosuppressive effect in models of cerebral malaria, decreasing edema and improving survival of afflicted mice, with corresponding inhibition of CD-8 T-cell degranulation [19,40]. DON similarly exerts robust anti-inflammatory effects a viral mouse model of encephalitis [28]. Interestingly, when DON treatment stopped, the inflammation resumed and rapidly progressed, leading to the death of mice [28]. The rebound inflammation seen in viral encephalitis suggests that clinical use of DON might, similar to high-dose cyclophosphamide, alter the microenvironment in ways that could be manipulated to enhance the immune response [17]. JHU-083 alters microglial metabolism by suppressing glutaminase activity [50]. Changes in microglial/macrophage metabolism may affect the polarity of these cells and alter the immune microenvironment, contributing to or thwarting an immune response [34].

These studies indicate that DON/JHU-083 has a profound impact on both innate and adaptive immunity. Demonstrating that the anti-tumor effects of JHU-083 are preserved in the presence of an intact immune system therefore lends important translational strength to our findings. Many preclinical studies are unable to include complementary data in immune intact systems due to a lack

of appropriate models, and this may represent an overall obstacle to clinical translation. Our immune-intact model presents an opportunity to further investigate the use of novel metabolism-altering therapies along with immunotherapy in medulloblastoma.

DON is a naturally occurring antibiotic first isolated from *Streptomyces* species in the 1950s [13]. It has been used in early phase clinical trials, including a phase I clinical trial in pediatric patients, however, it has never been systematically tested against MYC-expressing malignancies [41]. DON is known to target multiple enzymes that use glutamine, including glutaminase (GLS), asparagine synthetase, and phosphoribosylformylglycinamidine synthase [1,42]. The well-established linkages between MYC and glutamine metabolism in general [8], and the increased mortality observed in pediatric medulloblastoma patients with evidence of highly active tumor glutamine metabolism, [45] led us to hypothesize that DON prodrugs would be active against MYC-driven medulloblastoma models. We found that DON prodrugs were active at concentrations nearly 10-fold lower (10 uM *vs* 900 uM) than that recently reported for DON against the non-MYC medulloblastoma cell lines UW228 and DAOY [32], suggesting that the presence of the MYC proto-oncogene renders cells highly sensitive to glutamine metabolic inhibition. Indeed, DON prodrug concentrations that are highly lethal to neural stem cells engineered to express MYC have no effect on similar cerebellar stem cells immortalized with SV40. The addition of MYC to neural stem cells is associated with increased GLS expression, suggesting an increased reliance on glutamine metabolism downstream of MYC, consistent with prior reports demonstrating that MYC broadly regulates glutamine metabolism [18].

Although DON is currently not available for clinical use, the safety profile of this drug in pediatric patients was superior to that of traditional chemotherapy. The maximum tolerated dose (MTD) of DON was not reached in the pediatric phase I trial, with the trial terminating at a dosage level of 520 mg/m^2 administered twice weekly after enrolling 17 patients [41]. Our effective dose of 20 mg/kg twice weekly of JHU-083 in mice is equivalent to 2.4 mg/kg in a child or approximately 60 mg/m^2 [38], indicating that our dosing schedule is significantly below the MTD of DON in pediatric patients. Major side-effects in the pediatric phase I trial of DON were nausea and vomiting, which was well controlled with anti-emetic medication [41]. Orally bioavailable DON prodrugs provide a path for clinical development of glutamine antagonists for use in pediatric patients. We here demonstrate that oral JHU-083 provides robust delivery of DON into diverse brain regions in the mouse as well as significant activity against multiple models of MYC-driven medulloblastoma. We anticipate that on-going engineering of DON prodrugs will enhance brain penetration and reduce systemic exposure, thereby further broadening the therapeutic index.

Supplementary data to this article can be found online at https://doi.org/10.1016/j.tranon.2019.05.013.

References

[1] Ahluwalia GS, Grem JL, Hao Z, and Cooney DA (1990). Metabolism and action of amino acid analog anti-cancer agents. *Pharmacol Ther* **46**, 243–271.

[2] Archer TC, Ehrenberger T, Mundt F, Gold MP, Krug K, Mah CK, Mahoney EL, Daniel CJ, LeNail A, and Ramamoorthy D, et al (2018). Proteomics, Post-translational Modifications, and Integrative Analyses Reveal Molecular Heterogeneity within Medulloblastoma Subgroups. *Cancer cell* **34**(e398), 396–410.

[3] Bettencourt IA and Powell JD (2017). Targeting Metabolism as a Novel Therapeutic Approach to Autoimmunity, Inflammation, and Transplantation. *J Immunol* **198**, 999–1005.

[4] Bhutia YD, Babu E, Ramachandran S, and Ganapathy V (2015). Amino Acid transporters in cancer and their relevance to "glutamine addiction": novel targets for the design of a new class of anticancer drugs. *Cancer Res* **75**, 1782–1788.

[5] Bowers DC, Liu Y, Leisenring W, McNeil E, Stovall M, Gurney JG, Robison LL, Packer RJ, and Oeffinger KC (2006). Late-occurring stroke among long-term survivors of childhood leukemia and brain tumors: a report from the Childhood Cancer Survivor Study. *J Clin Oncol* **24**, 5277–5282.

[6] Brabetz S, Leary SES, Grobner SN, Nakamoto MW, Seker-Cin H, Girard EJ, Cole B, Strand AD, Bloom KL, and Hovestadt V, et al (2018). A biobank of patient-derived pediatric brain tumor models. *Nat Med* **24**, 1752–1761.

[7] Cho YJ, Tsherniak A, Tamayo P, Santagata S, Ligon A, Greulich H, Berhoukim R, Amani V, Goumnerova L, and Eberhart CG, et al (2011). Integrative genomic analysis of medulloblastoma identifies a molecular subgroup that drives poor clinical outcome. *J Clin Oncol* **29**, 1424–1430.

[8] Dang CV (2011). Therapeutic Targeting of Myc-Reprogrammed Cancer Cell Metabolism. *Cold Spring Harb Symp Quant Biol* **76**, 369-367.

[9] Dang CV (2012). MYC on the path to cancer. *Cell* **149**, 22–35.

[10] Dang CV, Hamaker M, Sun P, Le A, and Gao P (2011). Therapeutic targeting of cancer cell metabolism. *J Mol Med (Berl)* **89**, 205–212.

[11] Dang CV, Le A, and Gao P (2009). MYC-induced cancer cell energy metabolism and therapeutic opportunities. *Clin Cancer Res* **15**, 6479–6483.

[12] DeBerardinis RJ, Mancuso A, Daikhin E, Nissim I, Yudkoff M, Wehrli S, and Thompson CB (2007). Beyond aerobic glycolysis: transformed cells can engage in glutamine metabolism that exceeds the requirement for protein and nucleotide synthesis. *Proc Natl Acad Sci U S A* **104**, 19345–19350.

[13] Dion HW, Fusari SA, Jakubowski ZL, Zora JG, and Bartz QR (1956). 6-Diazo-5-oxo-L-norleucine, a new tumor-inhibitory substance. II. Isolation and characterization. *J Am Chem Soc* , 3075–3077.

[14] Eberhart CG and Burger PC (2003). Anaplasia and grading in medulloblastomas. *Brain Pathol* **13**, 376–385.

[15] Ellenberg L, Liu Q, Gioia G, Yasui Y, Packer RJ, Mertens A, Donaldson SS, Stovall M, Kadan-Lottick N, and Armstrong G, et al (2009). Neurocognitive status in long-term survivors of childhood CNS malignancies: a report from the Childhood Cancer Survivor Study. *Neuropsychology* **23**, 705–717.

[16] Friedman DL, Whitton J, Leisenring W, Mertens AC, Hammond S, Stovall M, Donaldson SS, Meadows AT, Robison LL, and Neglia JP (2010). Subsequent neoplasms in 5-year survivors of childhood cancer: the Childhood Cancer Survivor Study. *J Natl Cancer Inst* **102**, 1083–1095.

[17] Galluzzi L, Buque A, Kepp O, Zitvogel L, and Kroemer G (2015). Immunological Effects of Conventional Chemotherapy and Targeted Anticancer Agents. *Cancer Cell* **28**, 690–714.

[18] Gao P, Tchernyshyov I, Chang TC, Lee YS, Kita K, Ochi T, Zeller KI, De Marzo AM, Van Eyk JE, and Mendell JT, et al (2009). c-Myc suppression of miR-23a/b enhances mitochondrial glutaminase expression and glutamine metabolism. *Nature* **458**, 762–765.

[19] Gordon EB, Hart GT, Tran TM, Waisberg M, Akkaya M, Kim AS, Hamilton SE, Pena M, Yazew T, and Qi CF, et al (2015). Targeting glutamine metabolism rescues mice from late-stage cerebral malaria. *Proc Natl Acad Sci U S A* **112**, 13075–13080.

[20] Hanaford AR, Archer TC, Price A, Kahlert UD, Maciaczyk J, Nikkhah G, Kim JW, Ehrenberger T, Clemons PA, and Dancik V, et al (2016). DiSCoVERing Innovative Therapies for Rare Tumors: Combining Genetically Accurate Disease Models with In Silico Analysis to Identify Novel Therapeutic Targets. *Clinical cancer research : an official journal of the American Association for Cancer Research* **22**, 3903–3914.

[21] He XM, Wikstrand CJ, Friedman HS, Bigner SH, Pleasure S, Trojanowski JQ, and Bigner DD (1991). Differentiation characteristics of newly established medulloblastoma cell lines (D384 Med, D425 Med, and D458 Med) and their transplantable xenografts. *Lab Investig* **64**, 833–843.

[22] Hill RM, Kuijper S, Lindsey JC, Petrie K, Schwalbe EC, Barker K, Boult JK, Williamson D, Ahmad Z, and Hallsworth A, et al (2015). Combined MYC and P53 defects emerge at medulloblastoma relapse and define rapidly progressive, therapeutically targetable disease. *Cancer Cell* **27**, 72–84.

[23] Kaneko S and Yamanaka S (2013). To be immunogenic, or not to be: that's the iPSC question. *Cell Stem Cell* **12**, 385–386.

[24] King AA, Seidel K, Di C, Leisenring WM, Perkins SM, Krull KR, Sklar CA, Green DM, Armstrong GT, and Zeltzer LK, et al (2016). Long-term

neurologic health and psychosocial function of adult survivors of childhood medulloblastoma/PNET: a report from the Childhood Cancer Survivor Study. *Neuro-Oncology* **19**, 689–698.

[25] Kool M, Korshunov A, Remke M, Jones DT, Schlanstein M, Northcott PA, Cho YJ, Koster J, Schouten-van Meeteren A, and van Vuurden D, et al (2012). Molecular subgroups of medulloblastoma: an international meta-analysis of transcriptome, genetic aberrations, and clinical data of WNT, SHH, Group 3, and Group 4 medulloblastomas. *Acta Neuropathol* **123**, 473–484.

[26] Liu W, Le A, Hancock C, Lane AN, Dang CV, Fan TW, and Phang JM (2012). Reprogramming of proline and glutamine metabolism contributes to the proliferative and metabolic responses regulated by oncogenic transcription factor c-MYC. *Proc Natl Acad Sci U S A* **109**, 8983–8988.

[27] Lunt SY and Vander Heiden MG (2011). Aerobic glycolysis: meeting the metabolic requirements of cell proliferation. *Annu Rev Cell Dev Biol* **27**, 441–464.

[28] Manivannan S, Baxter VK, Schultz KL, Slusher BS, and Griffin DE (2016). Protective Effects of Glutamine Antagonist 6-Diazo-5-Oxo-l-Norleucine in Mice with Alphavirus Encephalomyelitis. *J Virol* **90**, 9251–9262.

[29] Mao XG, Hutt-Cabezas M, Orr BA, Weingart M, Taylor I, Rajan AK, Odia Y, Kahlert U, Maciaczyk J, and Nikkhah G, et al (2013). LIN28A facilitates the transformation of human neural stem cells and promotes glioblastoma tumorigenesis through a pro-invasive genetic program. *Oncotarget* **4**, 1050–1064.

[30] Martin AM, Nirschl CJ, Polanczyk MJ, Bell WR, Nirschl TR, Harris-Bookman S, Phallen J, Hicks J, Martinez D, and Ogurtsova A, et al (2018). PD-L1 expression in medulloblastoma: an evaluation by subgroup. *Oncotarget* **9**, 19177–19191.

[31] McKeehan WL (1982). Glycolysis, glutaminolysis and cell proliferation. *Cell Biol Int Rep* **6**, 635–650.

[32] Niklison-Chirou MV, Erngren I, Engskog M, Haglof J, Picard D, Remke M, McPolin PHR, Selby M, Williamson D, and Clifford SC, et al (2017). TAp73 is a marker of glutamine addiction in medulloblastoma. *Genes Dev* **31**, 1738–1753.

[33] Northcott PA, Korshunov A, Witt H, Hielscher T, Eberhart CG, Mack S, Bouffet E, Clifford SC, Hawkins CE, and French P, et al (2011). Medulloblastoma comprises four distinct molecular variants. *J Clin Oncol* **29**, 1408–1414.

[34] Palmieri EM, Menga A, Martin-Perez R, Quinto A, Riera-Domingo C, De Tullio G, Hooper DC, Lamers WH, Ghesquiere B, and McVicar DW, et al (2017). Pharmacologic or Genetic Targeting of Glutamine Synthetase Skews Macrophages toward an M1-like Phenotype and Inhibits Tumor Metastasis. *Cell Rep* **20**, 1654–1666.

[35] Pei Y, Moore CE, Wang J, Tewari AK, Eroshkin A, Cho YJ, Witt H, Korshunov A, Read TA, and Sun JL, et al (2012). An Animal Model of MYC-Driven Medulloblastoma. *Cancer Cell* **21**, 155–167.

[36] Raabe EH, Lim KS, Kim JM, Meeker A, Mao XG, Nikkhah G, Maciaczyk J, Kahlert U, Jain D, and Bar E, et al (2011). BRAF activation induces transformation and then senescence in human neural stem cells: a pilocytic astrocytoma model. *Clin Cancer Res* **17**, 3590–3599.

[37] Rais R, Jancarik A, Tenora L, Nedelcovych M, Alt J, Englert J, Rojas C, Le A, Elgogary A, and Tan J, et al (2016). Discovery of 6-Diazo-5-oxo-l-norleucine (DON) Prodrugs with Enhanced CSF Delivery in Monkeys: A Potential Treatment for Glioblastoma. *J Med Chem* **59**, 8621–8633.

[38] Reagan-Shaw S, Nihal M, and Ahmad N (2008). Dose translation from animal to human studies revisited. *FASEB J* **22**, 659–661.

[39] Ricardi U, Corrias A, Einaudi S, Genitori L, Sandri A, di Montezemolo LC, Besenzon L, Madon E, and Urgesi A (2001). Thyroid dysfunction as a late effect in childhood medulloblastoma: a comparison of hyperfractionated versus conventionally fractionated craniospinal radiotherapy. *Int J Radiat Oncol Biol Phys* **50**, 1287–1294.

[40] Riggle BA, Sinharay S, Schreiber-Stainthorp W, Munasinghe JP, Maric D, Prchalova E, Slusher BS, Powell JD, Miller LH, and Pierce SK, et al (2018). MRI demonstrates glutamine antagonist-mediated reversal of cerebral malaria pathology in mice. *Proc Natl Acad Sci U S A* **115**, E12024-12033.

[41] Sullivan MP, Nelson JA, Feldman S, and Van Nguyen B (1988). Pharmacokinetic and phase I study of intravenous DON (6-diazo-5-oxo-L-norleucine) in children. *Cancer Chemother Pharmacol* **21**, 78–84.

[42] Tarnowski GS, Mountain IM, and Stock CC (1970). Combination therapy of animal tumors with L-asparaginase and antagonists of glutamine or glutamic acid. *Cancer Res* **30**, 1118–1122.

[43] Weil AG, Wang AC, Westwick HJ, Ibrahim GM, Ariani RT, Crevier L, Perreault S, Davidson T, Tseng CH, and Fallah A (2016). Survival in pediatric medulloblastoma: a population-based observational study to improve prognostication. *J Neuro-Oncol* **132**, 99–107.

[44] Wells EM, Khademian ZP, Walsh KS, Vezina G, Sposto R, Keating RF, and Packer RJ (2010). Postoperative cerebellar mutism syndrome following treatment of medulloblastoma: neuroradiographic features and origin. *J Neurosurg Pediatr* **5**, 329–334.

[45] Wilson M, Gill SK, MacPherson L, English M, Arvanitis TN, and Peet AC (2014). Noninvasive detection of glutamate predicts survival in pediatric medulloblastoma. *Clinical cancer research : an official journal of the American Association for Cancer Research* **20**, 4532–4539.

[46] M. Wilson, S.K. Gill, L. MacPherson, M. English, T.N. Arvanitis, A.C. Peet, Non-invasive detection of glutamate predicts survival in pediatric medulloblastoma. Clinical cancer research : an official journal of the American Association for Cancer Research (2014a).

[47] Wise DR, DeBerardinis RJ, Mancuso A, Sayed N, Zhang XY, Pfeiffer HK, Nissim I, Daikhin E, Yudkoff M, and McMahon SB, et al (2008). Myc regulates a transcriptional program that stimulates mitochondrial glutaminolysis and leads to glutamine addiction. *Proc Natl Acad Sci U S A* **105**, 18782–18787.

[48] Yang L, Venneti S, and Nagrath D (2017). Glutaminolysis: A Hallmark of Cancer Metabolism. *Annu Rev Biomed Eng* **19**, 163–194.

[49] Zhu X, Nedelcovych MT, Thomas AG, Hasegawa Y, Moreno-Megui A, Coomer W, Vohra V, Saito A, Perez G, and Wu Y, et al (2019). JHU-083 selectively blocks glutaminase activity in brain CD11b(+) cells and prevents depression-associated behaviors induced by chronic social defeat stress. *Neuropsychopharmacology : official publication of the American College of Neuropsychopharmacology* **44**, 683–694.

[50] Zhu X, Nedelcovych MT, Thomas AG, Hasegawa Y, Moreno-Megui A, Coomer W, Vohra V, Saito A, Perez G, and Wu Y, et al (2019). JHU-083 selectively blocks glutaminase activity in brain CD11b(+) cells and prevents depression-associated behaviors induced by chronic social defeat stress. *Neuropsychopharmacology* **44**, 683–694.